Canadian Chemical Transactions Year 2015 | Volume 3 | Issue 3 | Page 340-353

Research Article

DOI:10.13179/canchemtrans.2015.03.03.0225

Dual Fluorescence of 4,4′-sulfonyldiphenol, 3,3'–dimethyl 4,4′-sulfonyldiphenol, 4,4′-sulfonyldibenzoic acid: Effects of Cyclodextrin Complexation

N. Rajendiran*, T. Mohandoss, J. Thulasidhasan

Department of Chemistry, Annamalai University, Annamalainagar - 608002, Tamilnadu, India

**Corresponding Author: Email: drrajendiran@rediffmail.com Tel.: +91 94866 28800*

Received: *August 24, 2015* ***Revised:*** *September 24, 2015* ***Accepted:*** *October 1, 2015* ***Published:*** *October 11, 2015*

Abstract: Absorption, steady state and time resolved fluorescence spectra of 4,4′-sulfonyldiphenol (SDP), 3,3'–dimethyl 4,4′-sulfonyldiphenol (DMSP), 4,4′-sulfonyldibenzoic acid (SDBA) were studied in the presence of α- and β-cyclodextrins. Both in water and CD, SDP and SDBA exhibit two emission maxima while DMSP exhibit three emission maxima. In β-CD, the rate of enhancement of longer wavelength (LW) emission is higher than that of shorter wavelength (SW) band, where as in α-CD the enhancement of SW is larger than that of LW. The normal Stokes shifted band was originated from the locally excited state and the large Stokes shifted band was due to the emission form a TICT state. In these molecules, the presence of OH or COOH groups at para position of the aromatic rings increase the coplanar geometry in the excited state. Semi-empirical quantum-mechanical calculations were also carried out to assign the encapsulation of the SDP, DMSP and SDBA. PM3 calculations show that most of the SDBA values are different from SDP and DMSP because the values are dependent on the size of the CD cavities and nature of the functional group of the guest.

Keywords: Sulphones, Cyclodextrin, Inclusion complex, TICT, Molecular modelling.

1. INTRODUCTION

Cyclodextrins (CDs) continue to attract considerable scientific attention due in part to the many spectacular applications related to guest-host and supramolecular chemistry. CDs can be described as shallow, truncated cones with a hydrophobic interior. The cavity selectively complexes guest molecules in aqueous solutions. Three of the most important cyclodextrins are α-CD, β-CD, and γ-CD in order of increased size. Because of its cavity size, cost and relative ease of chemical modification, the derivatives of α-CD and β-CD have been used commercially as drug carriers. An inhibiting property of β-CD has been its relatively low solubility in water compared with those of α- and γ-CDs that are nine and eleven times more soluble, respectively [1-5]. Therefore, a detailed understanding, based on molecular mechanisms, of the anomalous behavior of β-CD is important for catalytic, industrial, and pharmaceutical applications of CDs [4,5].

Diphenyl sulphone derivatives are found to be pharmaceutically and industrially important. Some of them are employed as antimalarial and antileprotic drugs [6-8] and also used in the preparation of industrially important products such as thermal recording materials, dyes, binding and vulcanizing agents [9]. The ground-state structure of the diphenyl sulphone molecules two rings has perpendicular to the plane defined by C-S--C bonds [10]. X-ray analysis of aminodiphenyl sulphone [10] also confirms the geometry of two phenyl rings. The possibility of d-orbital participation in an all-planar arrangement has been established by electron spin resonance data [11]. Further a number of diphenyl sulphone derivatives have long been known that high absorption leads to excited states with different electron density distributions depending on the nature and position of the substituents [12]. A dual luminescence in polar solvents due to twisted intramolecular charge transfer (TICT) states has been reported for 4,4'-diaminodiphenyl sulphone (4DADPS) and its dimethylamino derivative [13,14]. The temperature dependence of 2-aminodiphenyl sulphone (2ADPS) hasbeen carried out to find out the activation energy of charge delocalization or separation processes [15].

In middle of the 1990's, we have been studying the solvatochromic and prototropic effects of diphenyl sulphone [16,17] diphenyl [18,19], diphenyl ether [20,21] and with one or two electron-donating groups such as OH or NH_2. To continuation of our work, herein, we have studied the inclusion complexes of 4,4′-sulfonyldiphenol (SDP), 3,3'–dimethyl 4,4′-sulfonyldiphenol (DMSP), 4,4′-sulfonyldibenzoic acid (SDBA) (Fig. 1) with α-CD and β-CD. The main aims of the present study are: (i) to compare the effect of inclusion complexation of SDP, DMSP and SDBA molecules and (ii) the inclusion complexes whether increase or decrease the LW emission. The results are obtained by the UV-visible, steady state fluorescence, time resolved fluorescence measurement and molecular modelling methods.

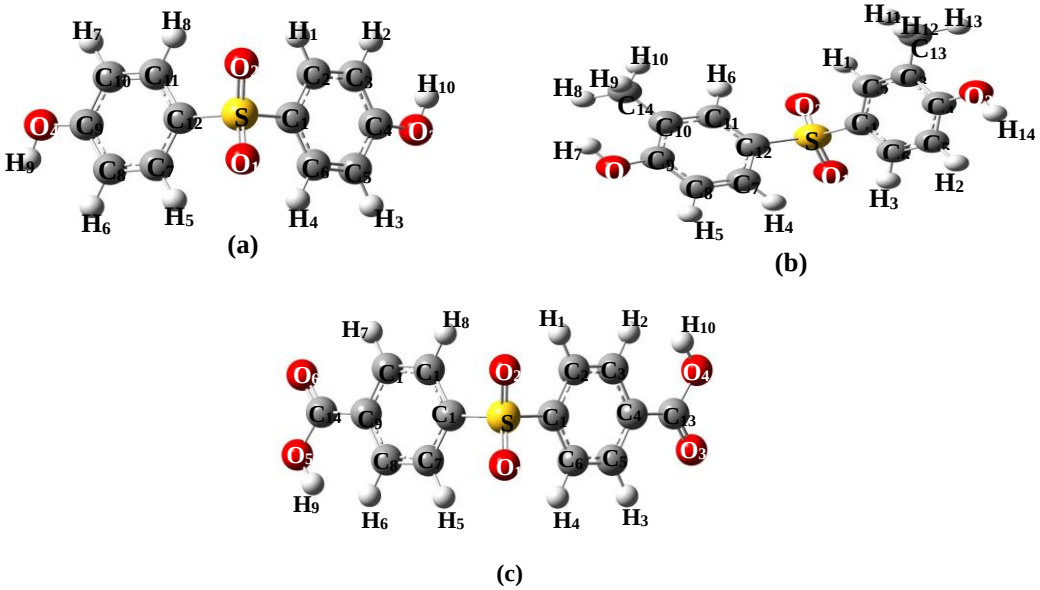

Figure 1. PM3 optimized structures of (a) 4,4′-sulfonyldiphenol (SDP), (b) 3,3'–dimethyl 4,4′-sulfonyldiphenol (DMSP) and (c) 4,4′-sulfonyldibenzoic acid (SDBA); colour of the atoms: grey – carbon, white – hydrogen, red – oxygen, yellow – sulphur.

2. EXPERIMENTAL SECTION

2.1. Materials

SDP, DMSP, SDBA, α-CD and β-CD were purchased from Sigma-Aldrich chemical company, USA and used without further purification. The purity of the compound was checked for similar fluorescence spectra when excited with different wavelengths. Triply distilled water was used for the preparation of aqueous solutions.

2.2. Preparation of CD Solution

The concentration of stock solution of the sulphones (SDP, DMSP and SDBA) was 2×10^{-3} M. The stock solution (0.2 ml) was transferred into 10 ml volumetric flasks. To this, varying concentration of CD solution (1×10^{-3} to 1×10^{-2} M) was added. The mixed solution was diluted to 10 ml with triply distilled water and shaken thoroughly. The final concentration of the sulphones in all the flasks was 4×10^{-5} M. The experiments were carried out at room temperature.

2.3. Instruments

Absorption spectral measurements were carried out with a Shimadzu UV 1601 PC model UV-visible spectrophotometer and steady-state fluorescence measurements were made by using a Shimadzu spectrofluorimeter model RF-5301. pH of the solution was measured in a Elico pH meter model LI-120. Fluorescence lifetime measurements were performed using a picoseconds laser and single photon counting setup from Jobin-Vyon IBH (Madras University, Chennai).

2.4. Molecular Modeling Studies

Theoretical calculations were performed with Gaussian 09W package. The initial geometry of SDP, DMSP, SDBA, α-CD and β-CD were constructed with the aid of Spartan 08 and then optimized by semi-empirical Parametric model 3 (PM3) method. The ground state geometry of guest molecules, α-CD, β-CD and inclusion complexes were optimized by using PM3 level of theory [22]. Due to large dimensions of the molecular structures, vibration frequency analysis was performed to characterize the local stationary points as the minima. Calculations were carried out in the gas phase, the effects of the solvent being not taken in the account. α-CD and β-CD was built up with α-D-glucopyranose residues, that were connected with other residues by α-(1-4)-glycoside oxygen bridges. Glycosidic oxygen atoms of CD were placed onto the XY plane and their centre was defined as the centre of the coordination system. Primary hydroxyl groups were placed pointing toward the positive Z axis. Inclusion complex was constructed from the PM3 optimized CD and guest molecules. Longer dimension of the guest molecule was initially placed onto the Z axis. The position of the guest was determined by the Z coordinate of one selected atom of the guest. The inclusion process was simulated by putting the guest on one end of CD and then letting it pass through the CD cavities. Since the semi-empirical PM3 method has been proved to be a powerful tool in the conformational study of CD inclusion complexes and has high computational efficiency [22], we selected semi-empirical PM3 method to study the inclusion process of CDs with the drug molecules.

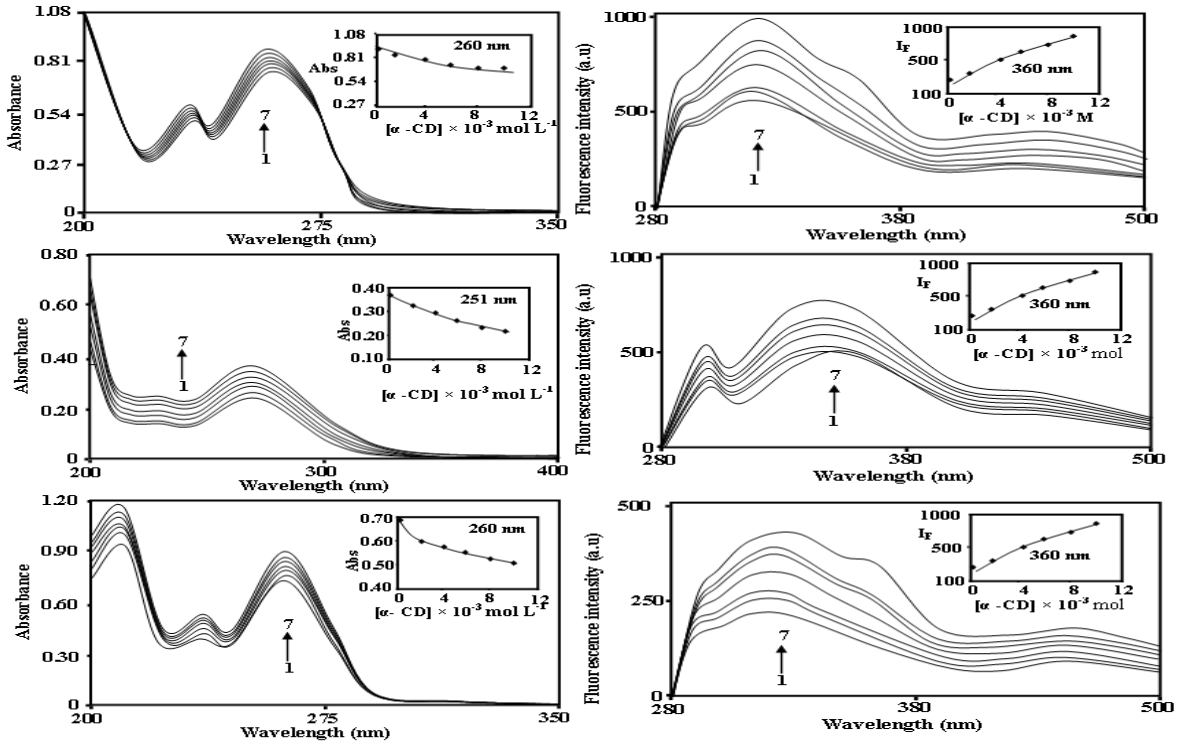

Figure 2. Absorbance and Fluorescence spectra of SDP, SDBA and DMSP in different α-CD concentrations (mol L^{-1}) : 1) 0, 2) 0.001, 3) 0.002, 4) 0.004, 5) 0.006, 6) 0.008, 7) 0.01. Insert figure Absorbance and fluorescence intensity *vs* α-CD concentrations.

3. RESULTS AND DISCUSSION

3.1. Absorption and fluorescence spectral studies

Absorption and fluorescence spectra of SDP, DMSP and SDBA with α-CD and β-CD in water are recorded and the relevant data listed in Table S1 (Supplementary data). Figures 2 and 3 display the absorption and fluorescence spectra of SDP, DMSP and SDBA as a function of α-CD and β-CD concentrations. In water, the absorption band maxima of SDP appears at ~258, 234 nm, DMSP appears at 261, 237 nm and SDBA shows at ~251, 234 nm. The absorption maximum of SDBA is slightly blue shifted than that of SDP and DMSP. This is due to presence of carboxylic anion in SDBA. Further, it is already reported [16,17] that in sulphones both phenyl rings are perpendicular to C-S-C plane and π-cloud of phenyl rings participate with the sulphur d- orbitals in the ground state. In these compounds both OH and COOH groups are placed symmetrically at para position to SO_2 group hence the solvent and CD effects are reduced giving rise to very small shifts in the absorption maxima [16,17].

No significant spectral shift was observed when the guest added into the α-CD and β-CD. Upon increasing the concentration of the CDs, the absorbance slightly increased at the same absorption wavelength. The slight increase in the absorbance with the addition of CDs can be attributed to the enhanced dissolution of the guest molecule through the detergent action of CD indicating the formation of guest/CD inclusion complexes.

A clear isosbestic point observed in SDP and DMSP suggest both molecules forms 1:1 inclusion complexes with CD, whereas in SDBA absence of isosbestic point may rule out the possibility of a single equilibrium involving 1:1 complexation between the drug and CD [23-29]. The possibilities are proposed for this deviation: (i) more than one guest molecule can be accommodated within a single CD cavity, (ii) due to the space restriction of CD cavity more than one type of complex each having 1:1 stoichiometry may be formed and (iii) the changes detected in the absorption spectra when CD is added to the guest solutions containing methanol (1%) can also made the interaction between both compounds. Since in this experiment the concentration of methanol is practically constant with respect to CD concentration it may affect the isosbestic point.

As can be seen from Table S1 (Supplementary data) the negative free energy change (ΔG) for of these complexes means that the binding process was spontaneous and thermodynamically favoured in the experimental temperature. The binding constant values for these molecules are significantly changed which reveals that different type of inclusion associated with β-CD. It is well known that substituents of aromatic rings capable of hydrogen bonding can bind the hydroxyl groups of the CD edges. The energy involved in such hydrogen bond interaction responsible for the higher/lower binding constants found, when compared to those of the substituted/unsubstituted molecules. The higher formation constant of the drugs implies that they are easily embedded in the β-CD cavity.

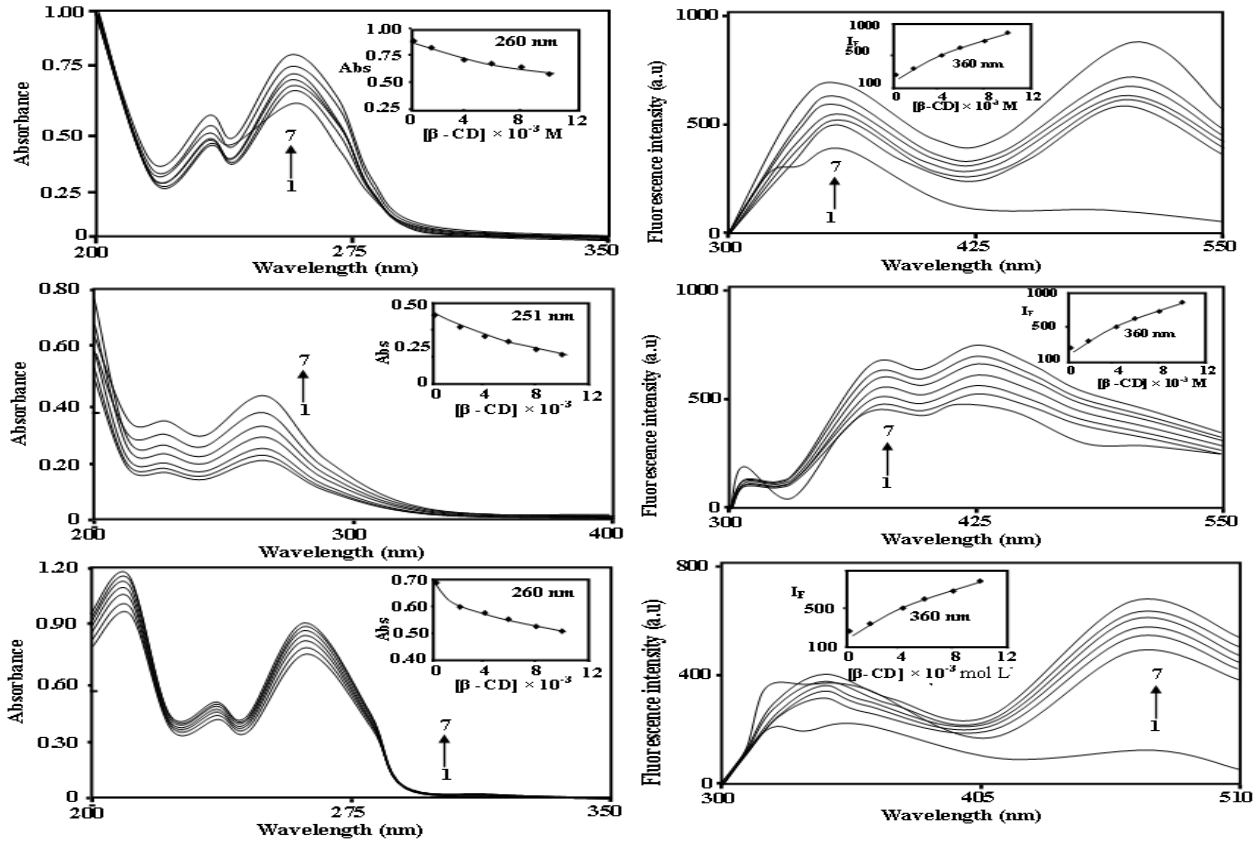

Figure. 3 Absorbance and Fluorescence spectra of SDP, SDBA and DMSP in different β-CD concentrations (M) $\lambda_{excitation}$ ~ 260 nm: 1) 0, 2) 0.001, 3) 0.002, 4) 0.004, 5) 0.006, 6) 0.008, 7) 0.01. Insert figure Absorbance and fluorescence intensity *vs* α-CD concentrations.

Figures 2 and 3 demonstrate the emission spectra of SDP, DMSP and SDBA in aqueous solution containing α-CD and β-CD at various concentrations. The effect of CD on the emission spectra of both molecules are more pronounced than the corresponding effect on the absorption spectra.

Both in water and CD, SDP and SDBA exhibit two emission maxima while DMSP exhibit three emission maxima. DMSP can emit relatively weak fluorescence in water whereas both emission bands are intensified in SDP and SDBA. Compared to aqueous solution the absorption and fluorescence intensities are larger in all the CDs solutions. The emission spectra of the guest molecules with β-CD are different from α-CD indicates different type of inclusion complexes formed.

The introduction of guests into aqueous CDs solution produced a red shift in the emission maxima of the sulphones. In α-CD, the enhancement of the shorter wavelength (SW) emission was higher than that of longer wavelength (LW) emission band while in β-CD it is vice versa; i.e., in β-CD, the rate of enhancement of LW emission is higher than that of SW band, where as in α-CD, the enhancement of SW is larger than that of LW. This can be clearly seen from looking at Figures 2 and 3. The above results indicate that, the above molecules form different type of inclusion complexes with α-CD and β-CD. Further, the above results suggest that the sulphone molecules are all entrapped deeply into the CD cavities. Further, the CD cavity provided an non-polar environment for the guest and motion of the guest inside the cavity was largely restricted. Thus, the enhanced rigidity of sulphone resulted in an increase in its fluorescence quantum yield.

With the addition of CD, both SW and LW emissions are slightly increased. Kim *et al* reported similar results in biphenyl molecules [30], when biphenyl formed complexation with β-CD, the excited state geometry may change toward coplanar conformation of the biphenyl becomes accessible. As like biphenyl, the coplanar geometry is also possible in these sulphone molecules because same functional groups (OH or COOH) present in the para position of the aromatic rings. In these molecules, the presence of OH or COOH groups at para position of the aromatic rings increase the coplanar geometry in the excited state (Fig 1). Further, the LW maxima increased in these molecules suggest that both aromatic rings are completely entrapped in the CD cavities, because the cavities provide a non-polar environment like cyclohexane. If SO_2 group encapsulated in the CD cavity, TICT is significantly reduced because the interaction between the SO_2 and water is decreased. Moreover, the LW fluorescence intensity increased in these molecules suggests that both aromatic rings are encapsulated in the non polar β-CD cavity. Further, if SO_2 group is present in the hydrophobic part of the CD cavity, it should decreases the TICT emission in the CD environment because it is well known that inside of the CD cavity provide non-polar environment. Therefore, we conclude, these drugs form 1:1 inclusion complex with CD and the interaction of SO_2 group is present in the hydrophilic environment hence TICT emission increased in the CD solution (Figures 2 and 3).

The association constant (K) and stoichiometry ratio of the inclusion complexes of SDP, DMSP and SDBA can be determined according to the Benesi-Hildebrand relation. Benesi-Hildebrand plot of these drug molecules are shown in Figs. 4, and the association constant for the inclusion complexes were calculated from slope and intercept of the plot.

3.2. Fluorescence lifetime

We have recorded the fluorescence lifetime of SDP, DMSP and SDBA in different environments. The typical time resolved fluorescence decay profile is presented in Table S1 and the spectra are shown in Fig. S1. The fluorescence decay behaviour of these molecules in water, α-CD and β-CD environments are

triexponential fit could yield acceptable results such behaviour may be attributed to the possible existence of different species i.e., locally excited state molecule (LE), hydrogen bonded and TICT species are formed. In these molecules, triexponential species observed in the SW and LW emission. In these environments TICT species have more lifetimes in the S_1 state compared to other two species. The average fluorescence lifetime at LW emission is increased in β-CD whereas SW emission lifetime is increased in the α-CD solutions. The increase in the fluorescence lifetime of three components of both molecules upon inclusion in the α-CD and β-CD is explained from a reduction in the polarity in the vicinity of the guest.

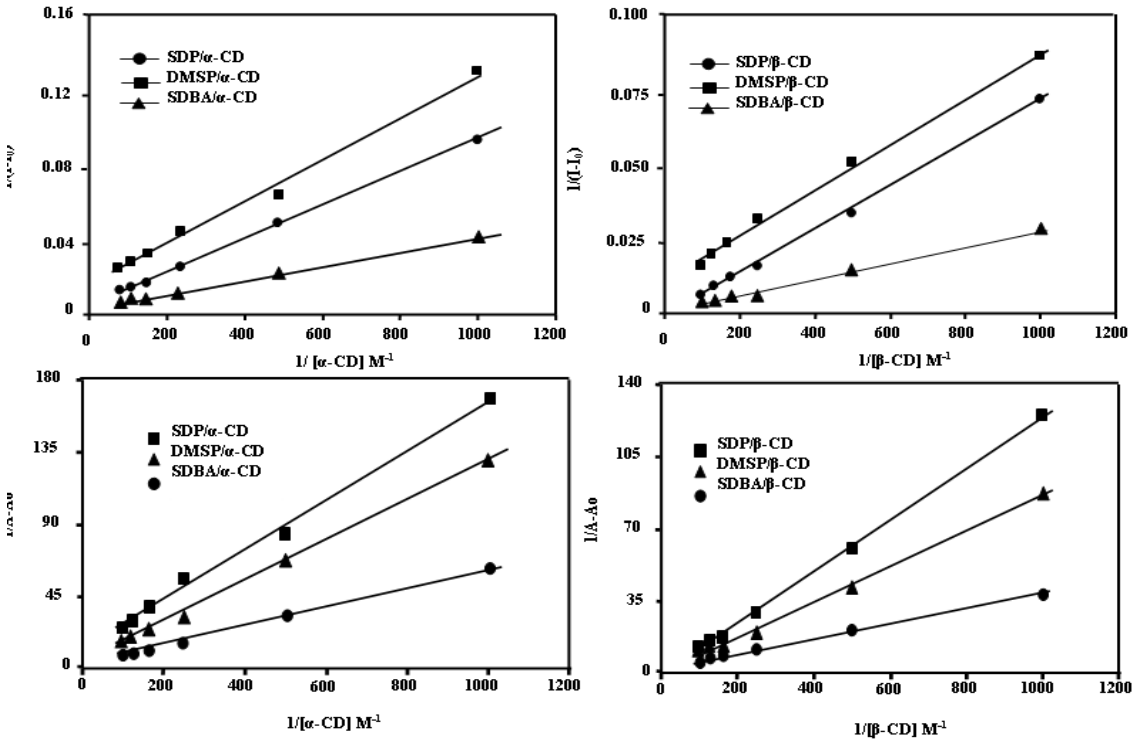

Figure 4. Benesi-Hildebrand plot for the complexation of SDP, DMSP and SDBA with α-CD and β-CD. Plot of $1/I-I_0$ versus 1/[CD] and $1/A-A_0$ vs. 1/[CD].

3.3. Molecular modelling

Semi-empirical quantum mechanical computations were executed in order to get additional information related to the structural features of the inclusion complexes between the SDP, DMSP and SDBA molecules with α-CD and β-CD. The optimized structure, bond distances, bond angles and most significant dihedral angles in SDP, DMSP and SDBA molecules before and after complexation calculated by PM3 method are presented in Tables S2 and S3. The optimized structure of the isolated drugs and the inclusion complexes are presented in Figs. 6 and S2. The corresponding frequencies were calculated to ensure that the obtained stationary points were the minima. All the semi-empirical calculations were performed using Gaussian 09W software.

As shown in Figs. 6 and S2, taking SDP, DMSP and SDBA with α-CD and β-CD system as an example, the energy decreases sharply from the starting point A (Z_A =9 Å; ZA being the

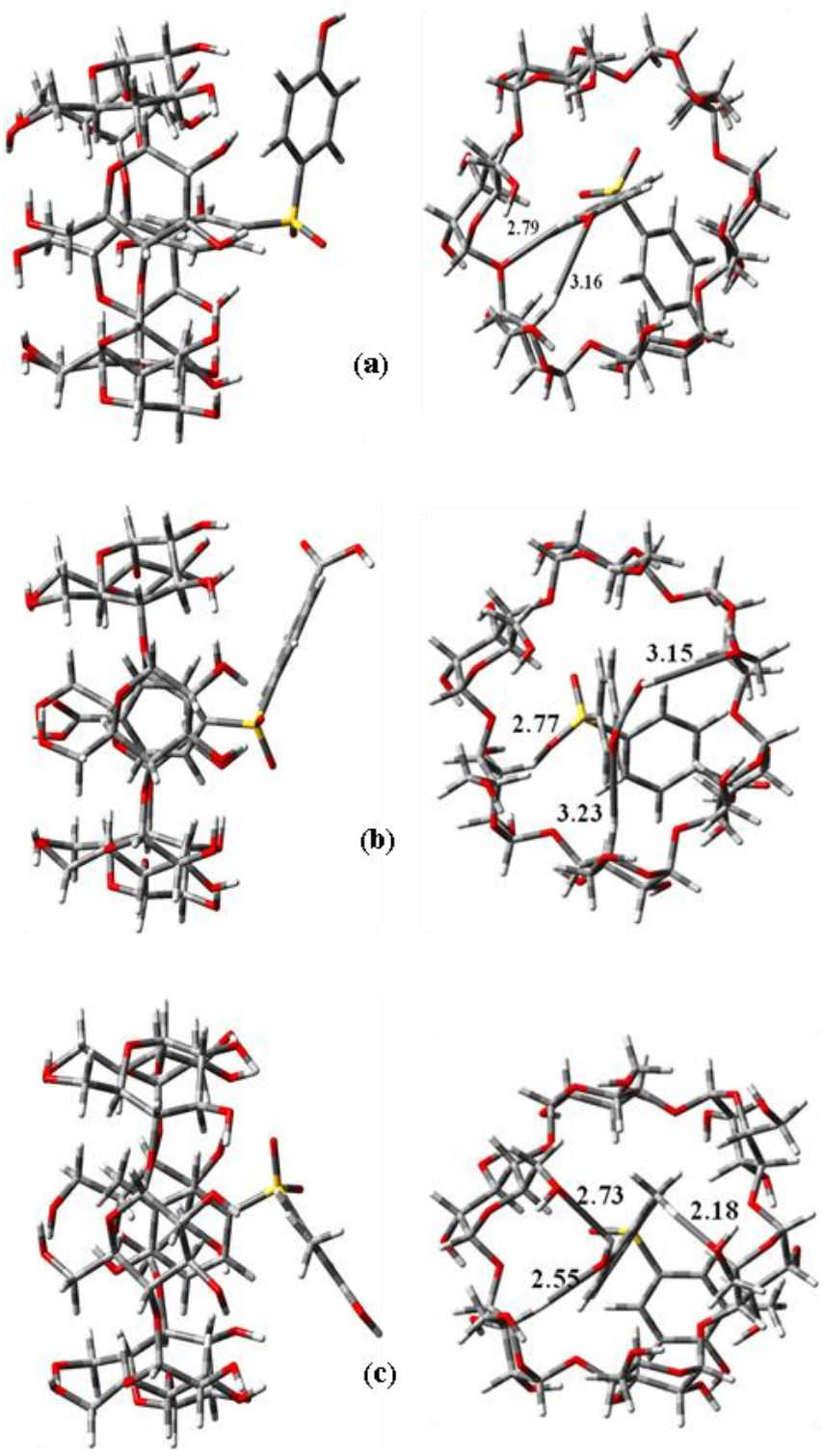

Figure 6. Upper and side views of PM3 optimized structures of (a) SDP/α-CD, (b) SDBA/α-CD, and (c) DMSP/α-CD inclusion complex.

Z coordinate of point A) until it reaches point B (Z_B = 1 Å), which is a local minimum. Then, the energy increases rapidly and achieves a local maximum at point C (Z_C =−1 Å). After that, the energy decreases again until it reaches point D (Z_D =−2 Å), the global minimum for the whole curve.

Fig 6 indicates that SDP, DMSP and SDBA with α-CD and β-CD could form the most stable inclusion complex in the Head-up pattern. Lastly, the energy increases until point E (Z_E = −9 Å). Similarly, we give a simple presentation of the energy changes obtained from SDP, DMSP and SDBA passing through α-CD and β-CD cavity from the wide side (Head-down). In Figs. 6 and S2, the energy decreases sharply from the starting point to reaching point B (Z_B = 2 Å), which is the global minimum of the whole curve indicates that SDP, DMSP and SDBA with α-CD and β-CD could form a stable inclusion complex in the Head-down pattern. Subsequently, the energy increases rapidly until reaching point C (Z_C =−8 Å). It can be seen that SDP, DMSP and SDBA with α-CD and β-CD can also form stable inclusion complexes for both Head-up and Head-down interactions.

The inner cavity diameter for α-CD is approximately 5.6 Å and β-CD is 6.5 Å and the height of all the CDs are 7.8 Å. In view of the shape and dimensions of CD (Figs. 6 and S2) the guest molecules cannot completely insert in the CD cavity. The vertical distance and the length of SDP, DMSP and SDBA is greater than the inside CD cavity and upper/lower rim of the CD. Hence, the aromatic ring may be partly present inside of the CD cavity. Further, the optimized structure of the inclusion complex by Gauss view method also confirmed one of the aromatic ring present in the hydrophobic part of the CD and SO_2 group present in the hydrophilic part of the CD cavity. The above finding confirmed SDP, DMSP and SDBA molecules are partially embedded in the CD cavity (Figs. 6 and S2). From the results, it is cleared that, after complexation the geometrical structures of the guest is completely altered. This alteration is very significant through the great variation of dihedral angels of the guest.

Considering the height and diameter of α-CD and β-CD, the guest molecules prefers to insert through the axial direction (long axis) (Figs. 6 and S2). In the present sulphones, if one aromatic ring encapsulated into the CD cavity, another phenyl ring should be projected outside of the cavity. For this orientation, one of the phenyl ring with OH or COOH is present outside of the CD cavity and interacts with the hydrophilic environment. PM3 calculations indicate these guests partially/completely included into the CD cavity and this is most favorable for the stability of the complex. The difference between the complex and the isolated guest and the CD energies values justify the formation of inclusion complex.

3.4. Driving force of complex formation

An important feature in complex stabilization is the ability of CDs to act as acid or weak Lewis base. This phenomenon can induce complex stabilization and is in close relationship with energies of HOMO and LUMO orbital of two guest molecules and the host. Different types of forces have been enclosed for their role in driving complex formation including electrostatic interactions, van der Walls contributions hydrogen bonding, release of conformational strain, exclusion of high energy water in the CD cavity and charge transfer interactions. In Table S2,

zero Mulliken population on the CD molecules can be observed suggesting charge transfer is not present between the host and guest molecules.

Tables S2 and S3 show most of the SDBA values are different from SDP and DMSP. This is because the values are dependent on the size of the CD cavities and nature of the functional group of the guest [31]. That is, the interaction is more sensitive to the nature of the functional group and the CD in the complexation. It is well known that the van der Waals force including the dipole–induced dipole interactions are proportional to the distance between the drugs and the wall of the CD cavities and to the polaraizabilities of the two components. The interaction of the phenyl ring with the CD would play an important role, because phenyl moiety may achieve a maximum contact area with the internal surface of the CD cavities.

Tables S2 and S3 values shows inclusion of SDP, DMSP and SDBA with CDs are also affected by hydrophobic and electronic interactions [32]. CDs have a permanent dipole [33] hence the primary hydroxy end is positive and the secondary hydroxy end is negative in the glucose units of CDs. The constancy of binding by hydrophobic communication is partly the result of van der Waals force but is mostly due to the effects of entropy produced on the water molecules [34]. In aqueous solution, hydrophobic guests are controlled by the water shell formed by the hydrogen bonding network [35,36]. It has a strong tendency to break down the water cluster and penetrate the non-polar cavity of the CD. The association constants for the inclusion of SDP, DMSP and SDBA with CDs were observed to be proportional to the substituent hydrophobic constant of the guest.

Figs. 6 and S2 for the complexes indicate that the interactions of hydrogen atoms of SDP, DMSP with CD are much stronger than SDBA because in SDBA, the presence of carboxylic anion prevents the hydrogen bond formation. The polar groups in the SDP, DMSP and SDBA molecules are determined by the inclusion process. The possible hydrogen bonds between the CD and the guests are shown in Figs. 6 and S2. The H-bond is defined as C=O···H (or) O–H···O with the distance between O and H being less than 3.0 Å. The H-bond lengths range from 2.18 to 3.00 Å in the structures, which fall just within the reported length range for H-bonds. The hydrogen bonding interactions are found to be the most important energetic factors that facilitate formation of the inclusion complex. Figs. 6 and S2 shows the hydrogen bonding interactions also play major roles in the inclusion complexation of CDs. The hydrogen bonds separate attractive forces, causing complex stabilization and can be considered as the driving force of the complexation process. These data indicate that intermolecular H-bonds play an important role in the stability of the inclusion complexes. In general, CD non-polar inner cavity is favours the non polar part of the guest. Therefore we concluded, the hydrogen bonding interaction, van der Waals interaction and breaking of the water cluster around this polar guest compound (drugs) mainly dominate driving force for the inclusion complex formation.

3.5. Thermodynamics parameters

To investigate the thermodynamics of the inclusion process, binding energies (ΔE), Gibbs energy changes (ΔG), enthalpy changes (ΔH) and entropy changes (ΔS) for SDP, DMSP and SDBA with α-CD and β-CD and most stable inclusion complexes are summarized in Table S2. Both theoretical and

experimental free energy change values of the inclusion complex were calculated from the formation constant (K). The experimental and theoretical ΔG values for the formation of the inclusion complexes are given in Tables S2 and S3. As can be seen from the Tables, the experimental ΔG value is negative which suggests that the inclusion proceeded simultaneously at 303 K. The experimental results are indicating that the inclusion reaction of SDP, DMSP and SDBA with α-CD and β-CD are an exothermic process.

The minimal energy of the molecular geometries was characterized by means of the stabilization energy (ΔE) between guest and the β-CD, according to eqn:

$$\Delta E = E_{complex} - (E_{CD} + E_{guest}) \quad (1)$$

where $E_{complex}$, E_{guest} and E_{CD} represent the heat of formation of the complex, free guest and free CD respectively. The magnitude of the energy change variation indicates the nature of the driving force involved in the complexation process. More negative is the stabilization energy, more thermodynamically favorable is the formation of the inclusion complex. The stabilization energy for each angle rotation at the starting point Z = 0 leads to exclusively negative values, which reveals that the energy of the complex is consistently lower than the sum of the isolated host and guest molecule energies. This indicates a high probability of complex formation, with guest completely included in the CD cavity. The binding energy for the guest – α-CD complex is lower than guest – β-CD complex.

PM3 calculations show that the E_{HOMO}-E_{LUMO} energy levels (Fig S3) and heat of formation calculations for the complexes are lower than those for isolated molecules. These calculations express that the energies of the complexation are lower than those for isolated host and guest. These calculations indicate that the stability of guest–α-CD complex is lower than guest–β-CD inclusion complex. The polarity of the CD cavity decreases after the guest enters into the CD cavity. As listed in Table S2, the dipole moment of the α-CD is 11.34, β-CD is 12.29 D, and the guest –CD is lower than the dipole moment for isolated CD. The above quantum mechanical calculation values show a strong correlation with the complexation behaviour.

The data in Table S2 indicate that the inclusion complex is more stable, which can be explained as follows: β-CD having the optimal size for its internal cavity (7.8Å) to encase the guest molecules. The standard formation enthalpies (ΔH°) of the inclusion complexes indicate that the formation reactions for the two complexes are weak exothermic processes. Negative standard Gibbs energy change (ΔG°) values indicate that the formations of all the complexes are spontaneous processes. The entropy effect (ΔS°) for the formation of the inclusion complexes are positive and has very little contribution to the negative value of the standard Gibbs energy than the heat effect. The positive entropy effect may be due to the combined results of the host-guest reaction (negative contribution to entropy) and releasing of water molecules from the cavity (positive contribution to entropy). Finally, formation of the inclusion complexes is enthalpy-entropy synergistically driven processes.

Further, the binding energies (ΔE) of the complexes formed by SDP, DMSP and SDBA passing through the cavity of CD from its wide side are about 10 $kJmol^{-1}$ lower than those approaching from the narrow side. Thus, it is predicted that the guests are favoured to enter the cavity of CD from its wide side. The negative ΔH and positive ΔS values suggest that formation of the inclusion complexes is an entropy-driven process. However, the experimental data indicate that formation of the inclusion complexes are enthalpy-entropy driving processes. The theoretical free energy values are different from experimental value is due to solvent effect. Unfortunately, because of limitations in the calculation ability of our computer and the large molecular size of CD calculations for these systems could not be performed for aqueous solutions. However, it is observed that the solvent effect on the host-guest interactions easily

changes the inclusion reaction from a non-spontaneous process in the gas phase to a spontaneous one in the aqueous phase. The host-guest interaction causes an enthalpy-entropy compensating process in the gas phase whereas the same interaction causes an enthalpy-entropy co-driven process in aqueous solution, because inclusion complexation releases a number of water molecules from the cavity of the CDs.

Generally, the inclusion process is associated with a relatively large negative value of ΔH while the ΔS can be either positive or negative. The hydrophobic interactions are related to a slightly positive ΔH and positive ΔS indicating that the process is entropy driven. The positive ΔS values are due to the breaking of highly ordered aqueous rich environments surrounding the hydrophobic part of the guest molecules upon binding the CD. In the present case, the obtained results indicate that the inclusion of guest in the CD in aqueous solution is favoured by both the enthalpy (ΔH >0) and entropy (ΔS > 0) terms.

4. CONCLUSION

The following conclusions can be drawn from the above studies: Dual emission observed in CD solutions suggested that the energy of the ICT state is lower than that of the locally excited state. The normal Stokes shifted band was originated from the locally excited state and the large Stokes shifted band was due to the emission from a intramolecular charge transfer (TICT) state. The ratio of the TICT emission to the normal emission increased with β-CD concentration, while it was constant upon addition of α-CD. This behavior is in accordance with CD dependent decay times of the TICT and normal emissions, indicating the formation of different 1:1 guest/CD inclusion complexes. The rise time for the TICT emission increased with β-CD concentration, whereas no rise time was observed in the case of the α-CD complex. PM3 calculations suggests the hydrogen bonding interactions also play major roles in the inclusion complexation of CDs.

ACKNOWLEDGEMENTS

This work was supported by the Council of Scientific Industrial Research, New Delhi, India [No. 01(2549)/12/ EMR-II] and University Grants Commission, [F. No. 41-351/2012 (SR)] New Delhi, India.

SUPPLEMENTARY INFORMATION

Supplementary data associated with this article can be found online

REFERENCES

[1] Naidoo, K. J.; Chen, J. Y. J.; Jansson, J. L. M.; Widmalm, G.; Maliniak. A. Molecular properties related to the anomalous solubility of β-cyclodextrin. *J. Phys. Chem. B.* **2004**, *108*, 4236-4238.

[2] Szejtli, J. Introduction and general overview of cyclodextrin chemistry. *Chem. Rev.* **1998**, *98*, 1743-1753.

[3] Stezowski, J. J.; Parker, W.; Hilgenkamp, S.; Gdaniec, M. Pseudopolymorphism in tetradeca-2,6-O-methyl-beta-cyclodextrin: The crystal structures for two new hydrates-conformational variability in the alkylated beta-cyclodextrin molecule. *J. Am. Chem. Soc.* **2001**, *123*, 3919-3926.

[4] Starikov, E. B.; Brasicke, K.; Knapp, E. W.; Saenger, W. Negative solubility coefficient of methylated cyclodextrins in water: A theoretical study. *Chem. Phys. Lett.* **2001**, *336*, 504-510.

[5] Dodziuk, H. Rigidity versus flexibility. A review of experimental and theoretical studies pertaining to the cyclodextrin nonrigidity. *J. Mol. Struct.* **2002**, *614*, 33-45.

[6] Lee, S. H.; Chung, U. T.; Kang, Y. K. Conformational analysis of some antibacterial agent 4-aminodiphenyl sulfones. *Arch. Pharmacol. Res.* **1990**, *13*, 43-50.

[7] Errol, Z.; Beth, A.; Steve, H.; Timothy L.; and Kristien, M. Salmonella Mutagenicity Tests: V. Results from the Testing of 311 Chemicals. *Environ. Mol. Mutagen.* **1992,** *19*, 21-41.

[8] Ishida, S.; Hamada, K.; Yagi K.; and Seino, M. Comparing the anticonvulsive effects of dapsone on amygdala-kindled seizures and hippocampal-kindled seizures in rats. *Acta Neurol. Scand*. **1992**, *85*, 132-135.

[9] Lesbats C.; and Lichanot, A. Capacites calorifiques de durcisseurs amines et resines epoxydes, *Thermochim. Acta*, **1987**, *109*, 317-329.

[10] Dickinson, C.; Stewart J. M.; and Ammon, H. L. The X-ray crystal structure of the antimalarial and antileprotic drug, 4,4′-diaminodiphenyl sulphone. *J. Chem. Soc. Chem. Commun.* **1970,** *15*, 920-925.

[11] Kaiser, E. T.; and Eargle, D. H. Conjugative Effects of Sulfur in Several Aromatic Anion-Radicals. *J. Am. Chem. Soc.* **1963**, *85*, 1821-1823.

[12] Fehenel, E. A.; Carmak, M. The Ultraviolet Absorption Spectra of Organic Sulfur Compounds. IV. Substituted Phenyl Sulfones. *J. Am. Chem. Soc.*, **1950**, *72*, 1292-1296.

[13] Rettig, W.; and Chandross, E. A.; *J. Am. Chem. Soc*. Dual fluorescence of 4,4'-dimethylamino- and 4,4'-diaminophenyl sulfone. Consequences of d-orbital participation in the intramolecular charge separation process. **1985,** 107, 5617-5624.

[14] Su S. G.; and Simon, J. D. *J. Phys. Chem.* Solvent dynamics and twisted intramolecular charge transfer in bis(4-aminophenyl) sulfone. **1986**, *90*, 6475-6479.

[15] Barigelletti, F. Temperature dependence of the luminescence of 2-aminophenyl phenylsulphone in polar solvents. *J. Chem. Soc. Faraday Trans*. **1987**, *83*, 1567-1576.

[16] Rajendiran, N.; Swaminathan, M. Photophysical behaviour of 4,4-dihydroxydiphenyl sulphone. *Indian J. Chem.* **1996**, *35A*, 385–389.

[17] Rajendiran, N.; Swaminathan, M. Solvatochromism and prototropism of diaminodiphenyl sulphones and 2-aminodiphenyl sulphone-A comparative study by electronic spectra. *J. Photochem. Photobiol. A: Chem.* **1995**, *90*, 109-116.

[18] Rajendiran, N.; Swaminathan, M. Photo luminescence of 4,4’-diaminodiphenyl. *Bull. Chem. Soc. Japan*. **1995**, *68*, 2797-2802.

[19] Kalaiyarasan, K.; Rajendiran, N.; Swaminathan, M. Photoluminescence of 2-hydoxybiphenyl and its methyl derivative, *Indian J. Chem.* **1994**, *33A*, 335–37.

[20] Rajendiran, N.; Swaminathan, M. Spectral characteristics of 4-aminodiphenyl ether in different solvents and various pH. *J. Photochem. Photobiol. A: Chem.* **1996**, *93*, 103-108.

[21] Rajendiran, N.; Swaminathan, M. Unusual spectral shifts of bis(4-amino phenyl) ether. *Bull. Chem. Soc. Japan*, **1996**, *69*, 2447–2452.

[22] Rafati, A. A.; Hashemianzadeh, S. M.; Nojini, Z. B.; Safarpour, M. A. Theoretical study of the inclusion complexes of α and β-cyclodextrins with decyltrimethylammonium bromide (DTAB) and tetradecyltrimethylammonium bromide (TTAB). *J. Mol. Liq.* **2007**, *135*, 153-157.

[23] Rajendiran, N.; Sankaranarayanan, R. K. Nanoscale self assembly of cyclodextrin capped 4-aminobenzophenone via non-covalent interactions. *J. Mol. Liq.* **2015**, *206*, 218-227.

[24] Rajendiran, N.; Venkatesh, G. Micrometer size rod like structure formed by secondary self assembly of omeprazole inclusion complexes with α- and β-cyclodextrins. *Spectrochim. Acta*, **2015**, *137*, 832-840.

[25] Rajendiran, N.; Mohandoss, T.; Sankaranarayanan, R. K. Nanostructures formed by cyclodextrin covered procainamide through supramolecular self assembly – Spectral and molecular modeling study. *Spectrochim. Acta*, **2015**, *136*, 875-883.

[26] Rajendiran, N.; Venkatesh, G.; Sankaranarayanan, R. K. Dual fluorescence of omeprazole: Effect of solvents and pH. *Phys Chem Liq*. **2014**, *52*, 738-750.

[27] Rajendiran, N.; Sankaranarayanan, R. K.; Venkatesh, G. Excimer emission in inclusion complexes of dibenzofuran and 5-dibenzosuberenone with α- and β-cyclodextrins. *Bull. Chem. Soc. Japan*, **2014**, *87*, 797-808.

[28] Rajendiran, N.; Mohandoss, T.; Thulasidhasan, J. Excimer Emission in Norepinephrine and Epinephrine drugs with α- and β-Cyclodextrins: Spectral and Molecular Modeling Studies. *J Fluorescence*. **2014**, *24*, 1003-1014.

[29] Rajendiran, N.; Venkatesh, G.; Saravanan, J. Encapsulation of thiazoresorcinol and thiazocresol dye within α- and β-CD cavities: Spectral and molecular modeling studies. *J Mol Stru*. **2014**, *1072*, 242-252.

[30] Cho, D. W.; Kim, Y. H.; Kong, S. G.; Yoon, M. Cyclodextrin effects on excited-state geometry change and intramolecular charge transfer of 4-biphenylcarboxylic acid. *J Phys Chem*. **1994**, *98*, 558 -562.

[31] Qing-Xiang Guo, Shuang-Hui-Luo, You-Cheng Liu. Substituent Effects on the Driving Force for Inclusion Complexation of α- and β-Cyclodextrin with Monosubstituted Benzene Derivatives. *J. Incl. Phenom. Macrocycl. Chem.* **1998**, *30*, 173-182.

[32] Davies, D. M.; Deary, M. E. Cooperativity and steric hindrance: important factors in the binding of α-cyclodextrin with para-substituted aryl alkyl sulfides, sulfoxides and sulfones. *J. Chem. Soc. Perkin Trans.* **1995**, *2*, 1287-1294.

[33] Wenz, G. Cyclodextrin as building blocks for supramolecular structure and functional units. *Angew Chem Int Ed Engl*. **1994**, *33*, 803-822.

[34] Inoue, Y.; Kitagawa M.; Hoshi, H.; Sakurai, M.; Chujo R. Geometry of α-cyclodextrin inclusion complex with m-nitrophenol deduced from quantum chemical analysis of carbon-13 chemical shifts. *J. Inclu. Phenomena and Macrocyclic Chem.* **1987**, *5*, 55-58.

[35] Sakurai, M.; Kitagawa, M.; Inoue. Y.; Chujo, R. A molecular orbital study of cyclodextrin (cyclomalto-oligosaccharide) inclusion complexes. III, dipole moments of cyclodextrins in various types of inclusion complex. *Carbohydr. Res.* **1990**, *198*, 181-191.

[36] Delaage, M.; in Delaage, M. (Ed) Molecular Recognition Mechanisms, Ch 1, VCH Publishers, New York, 1991.

The authors declare no conflict of interest

© 2015 By the Authors; Licensee Borderless Science Publishing, Canada. This is an open access article distributed under the terms and conditions of the Creative Commons Attribution license http://creativecommons.org/licenses/by/3.0